Neuroradiology (2015) 57:903–908
DOI 10.1007/s00234-015-1547-z

DIAGNOSTIC NEURORADIOLOGY

Evaluation of electrode position in deep brain stimulation by image fusion (MRI and CT)

I. Barnaure[1] · P. Pollak[2] · S. Momjian[3] · J. Horvath[2] · K. O. Lovblad[1] · C. Boëx[2] · J. Remuinan[4] · P. Burkhard[2] · M. I. Vargas[1]

Received: 17 March 2015 / Accepted: 21 May 2015 / Published online: 29 May 2015

Abstract
Introduction Imaging has an essential role in the evaluation of correct positioning of electrodes implanted for deep brain stimulation (DBS). Although MRI offers superior anatomic visualization of target sites, there are safety concerns in patients with implanted material; imaging guidelines are inconsistent and vary. The fusion of postoperative CT with preoperative MRI images can be an alternative for the assessment of electrode positioning. The purpose of this study was to assess the accuracy of measurements realized on fused images (acquired without a stereotactic frame) using a manufacturer-provided software.
Methods Data from 23 Parkinson's disease patients who underwent bilateral electrode placement for subthalamic nucleus (STN) DBS were acquired. Preoperative high-resolution T2-weighted sequences at 3 T, and postoperative CT series were fused using a commercially available software. Electrode tip position was measured on the obtained images in three directions (in relation to the midline, the AC-PC line and an AC-PC line orthogonal, respectively) and assessed in relation to measures realized on postoperative 3D T1 images acquired at 1.5 T.
Results Mean differences between measures carried out on fused images and on postoperative MRI lay between 0.17 and 0.97 mm.
Conclusion Fusion of CT and MRI images provides a safe and fast technique for postoperative assessment of electrode position in DBS.

Keywords Image fusion · CT · MRI · Deep brain stimulation · Electrode position

✉ M. I. Vargas
maria.i.vargas@hcuge.ch

[1] Department of Neuroradiology, Geneva University Hospital, Gabrielle Perret Gentil, 4, 1211 Geneva 14, Switzerland

[2] Department of Neurology, Geneva University Hospital, Geneva, Switzerland

[3] Department of Neurosurgery, Geneva University Hospital, Geneva, Switzerland

[4] Department of Radiology, Geneva University Hospital, Geneva, Switzerland

Introduction

In the past decades deep brain stimulation (DBS) has replaced lesional neurosurgery in the surgical treatment of Parkinson's disease (PD), based on the observation that high-frequency stimulation of target sites can imitate a lesion of the latter [1, 2]. While it is currently also used for other movement disorders (tremor, dystonia), pain and epilepsy, the largest treated group consists of PD patients—tens of thousands of patients having undergone surgery to this date [3]—and the most frequent target site is the subthalamic nucleus. Stimulation is achieved through implanted electrodes (leads composed of a platinum-iridium alloy).

Correct positioning of leads is essential for optimal clinical results and avoidance of adverse effects. While the excellent visualization of target structures on magnetic resonance imaging (MRI) would predispose it for the control of correct electrode positioning, reports of adverse events [4, 5] have reinforced concern about the safety of performing MRI in patients with implanted material (due to heating of electrodes and adjacent tissues in a magnetic field and possible functional disruption of the devices), although adverse events are rare in big cohorts when observing security guidelines [6, 7]. Existing

guidelines however include imaging at 1.5 T, a field strength which does not demonstrate the subthalamic nucleus as well and as reliably as 3 T, especially in the short acquisition times needed postoperatively for patient comfort. Some centers perform routine postoperative MRI for verification of electrode positioning while it is avoided in others; instead of routine imaging to verify localization of the electrodes, MRI may be reserved for other situations such as the appearance of new symptoms. In contrast, computed tomography (CT) offers good lead delineation and positional accuracy [8] but lacks sufficient soft tissue contrast for direct visualization of anatomical targets. An alternative combining the advantages of both imaging modalities and permitting to avoid the risks of postoperative MRI is the fusion of preoperative MRI and postoperative CT images for visualization of electrode position. Before implementation of such a protocol, the accuracy of measurements achieved by these means has to be verified. Previous studies with varying size and composition of patient cohorts and different methods for image acquisition and fusion have shown good accuracy of fusion and assessment of electrode position [9–11]. The purpose of this study was to compare measurements on fused images of postoperative CT and preoperative MRI (acquired under "standard conditions" without a stereotactic frame and analyzed using a manufacturer-provided simple software) and those on postoperative MRI (as current standard postoperative examination in our institution).

Materials and methods

Between June 2011 and January 2014, patients referred for DBS surgery had preoperative high-resolution MRI and postoperative MRI and CT, the latter in general both performed on the day after surgery as part of the current standard procedure in our institution (the CT realized first to rule out relevant bleeding and the MRI realized to evaluate electrode tip position). The postoperative CT was fused with the preoperative MRI to allow visualization of the electrode tip position. Results were compared with those obtained by evaluation of electrode tip position on the postoperative MRI. Results were retrospectively analyzed in order to evaluate the possibility to omit postoperative MRIs. This study was approved by the local ethical committee.

Subject group The subject group consisted of 23 patients with Parkinson's disease (12 female, 11 male, mean age 61 years) who underwent bilateral electrode placement for subthalamic nucleus (STN) DBS (with a total of 46 electrodes). Electrodes (Medtronic DBS lead model 3389, Medtronic, Minneapolis, MN, USA) were implanted under local anesthesia with use of a Leksell stereotactic frame (Elekta Instruments AB, Stockholn, Sweden) and anatomical (MRI and CT) and physiological targeting (microTargeting® electrode, Pt-Ir, FHC, Bowdoinham, ME, USA; with the Neurostar DBS-Guide and Neurobook systems, Tubingen, Germany). Based on microelectrode recordings, electrodes were considered as correctly located in the target region. Impulse generators (Medtronic Activa PC/SC, Minneapolis, MN, USA) were implanted and connected during a second surgical procedure on another day (after postoperative head MRI and CT).

Imaging Preoperative MRI was performed with a Siemens Trio 3.0 T scanner. The protocol included a high-resolution T2-weighted sequence with TE=223 ms, TR=2400 ms, field of view=450 mm^2, matrix=448, slice thickness=1.0 mm. Postoperative CT was performed with either a Siemens Somatom Definition Flash (Siemens, Erlangen, Germany) or a GE Discovery 750 HD (GE Healthcare, Milwaukee, USA) scanner with 120 kV and dose modulation (100–250 mA). Slice thickness differed between 0.6 and 1.25 mm. Postoperative MRI was performed on a Philips Achieva 1.5 T scanner and included a 3D T1-weighted sequence with TE=4.6 ms, TR=20 ms, field of view=250 mm^2, matrix=288, voxel size 0.9×1.28×0.9 mm.

Data analysis Preoperative high-resolution T2-weighted sequences obtained at 3 T and postoperative CT series were fused using a commercially available software (Integrated Registration, AW VolumeShare 4.6, GE Healthcare). The program performs a rigid-body registration using mutual registration with a two-pass-transform estimation (for translation and for rotation, using versor representation). Image alignment was visually assessed (Fig. 1). In cases in which alignment was not satisfactory by use of the "automatic alignment" option, it was achieved by use of the "manual alignment" option.

Electrode tip position was evaluated on the obtained images using multiplanar reformatting (MPR, Fig. 2). In a first step, the distance between the two electrodes tips was measured in axial and coronal planes to verify comparability of measures based on CT (CT being the sole input for electrode tip location on fused images) and postoperative MRI. Electrode tip location in relation to an anatomical landmark was determined in a second step. In the axial plane, the distance of each electrode tip from the midline was measured (mediolateral measure). In the sagittal plane, the distance of each electrode tip from the anterior commissure-posterior commissure (AC-PC) line (as projected on the image in which the electrode tip was visible) was recorded (craniocaudal measure) as well as the distance to a line perpendicular to the AC-PC line and passing through its midpoint (anteroposterior measure). Midline and AC-PC line were determined on the MRI part of the fused images. Lines toward the midline, the AC-PC line and the AC-PC line orthogonal were drawn in

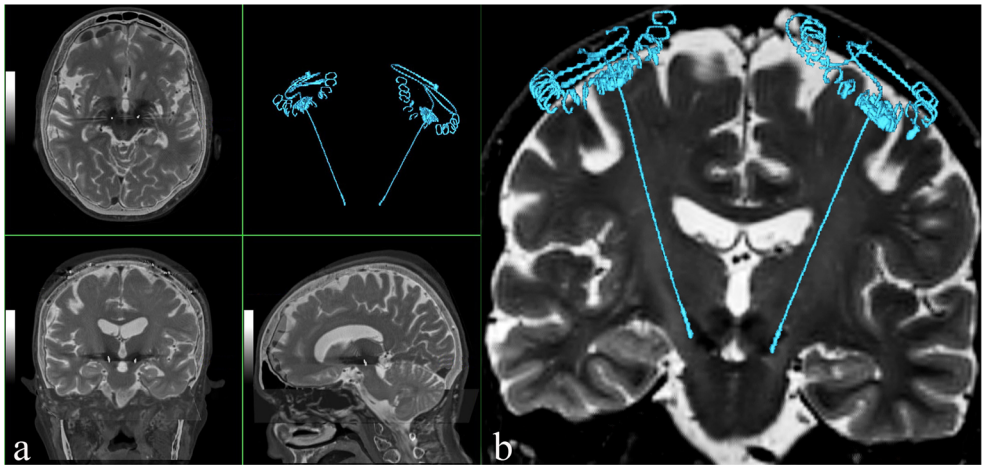

Fig. 1 Result of MRI and CT fusion. **a** Fused images in three planes using a preoperative high-resolution T2-weighted sequence and the bone algorithm reconstruction of postoperative CT. Electrodes are shown superimposed on detailed MRI-demonstrated anatomy (*top left*: axial, *bottom left*: coronal, *bottom right*: sagittal, *top right*: 3D volume rendering technique (VRT) presentation of electrodes). **b** 3D VRT presentation of electrodes from postoperative CT (*in blue*) superposed on preoperative MRI demonstrating electrode position

such a way that their intersection with the reference line (midline/AC-PC line/AC-PC line orthogonal) was orthogonal. The center of the electrode tip artifact was the starting point of the lines.

The same measurements as above (i.e., distance between electrode tips, mediolateral, craniocaudal, and anteroposterior measure) were done on the postoperative MRI 3D T1 sequence stored on our PACS, using multiplanar reformatting and the measuring tool of the PACS (OsiriX MD). Differences between distances obtained on these two datasets (fused images and postoperative MRI) were calculated and analyzed using a Student's *t* test.

Results

Automatic image alignment was satisfactory in 16/23 cases (70 %). In the remaining seven cases, satisfactory alignment was achieved by use of the manual alignment option. Slice

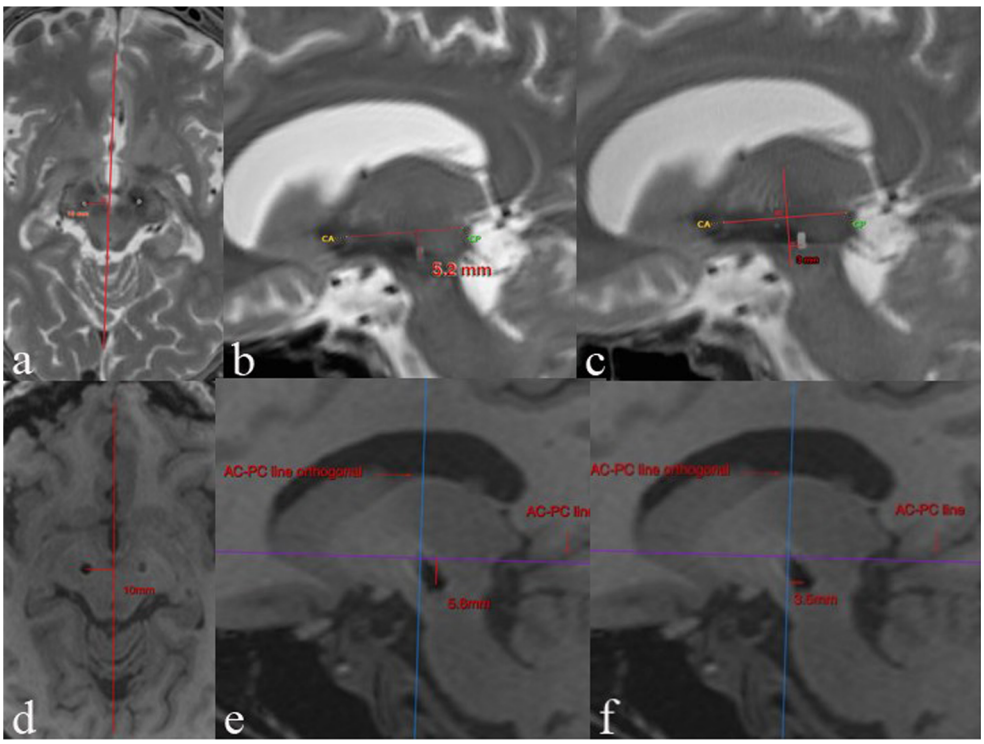

Fig. 2 Measures. *Top row*: Examples of the measures carried out on fused images using the fusion software: mediolateral distance (**a**), craniocaudal distance (**b**), anteroposterior distance (**c**). *Bottom row*: Examples of measures carried out on the postoperative MRI-reformatted 3D T1 sequence using PACS tools (different patient): mediolateral distance (**d**), craniocaudal distance (**e**), anteroposterior distance (**f**)

thickness of the postoperative CT or presence of motion artifacts did not influence upon the automatic alignment function.

The differences between measurements carried out on fused preoperative MRI/postoperative CT images and on postoperative MRI images are reported in Tables 1 and 2. The difference in distance between the electrode tips was 0.17 mm (SD 0.47; range 0.0–0.9) as measured in an axial plane and 0.38 (SD 0.57, range 0.1–1.3) in a coronal plane.

The difference in distance to the midline was 0.11 (SD 0.78, range 0.1–1.8) for the right and −0.17 (SD 0.78, range 0–1.8) for the left electrode on axial images (on coronal images, respectively, 0.47, SD 0.56, range 0–1.6 and −0.15, SD 0.49, range 0.1–1.1, not shown). The difference in distance to the AC-PC line (craniocaudal measure) was 0.73 (SD 0.86, range 0.0–2.6) for the right and 0.97 (SD 0.96, range 0.1–3.6) for the left electrode tip. Differences in anteroposterior distances were 0.67 (SD 1.27, range 0.1–4.6) and 0.51 (SD 0.97, range 0–3.7) for the right and left electrodes, respectively. The maximal differences (4.6 and 3.7) corresponded to measurements of one case in which automatic alignment did not work.

Differences were significant for measurements realized on sagittal and coronal images (p=0.0001 for craniocaudal left, 0.0005 for craniocaudal right, 0.0184 for anteroposterior left, 0.0116 for anteroposterior right, and 0.0038 for the distance between electrodes on coronal images, respectively).

Discussion

The results of this study in a relatively large and uniform cohort show that fusion of CT and MR images acquired under standard clinical conditions permits adequate measurements as compared to postoperative unfused MRI. Mean errors of 0.11 to 0.97 correspond to those found in other studies on the accuracy of measures acquired on fused images in STN DBS with use of different image acquisition and fusion protocols, as the acquisition with a stereotactic frame in place or the fusion of preoperative CT and postoperative MRI, using commercially available surgical or radiological workstation fusion protocols [10, 9] and are in an acceptable range with regard to target and electrode size.

Table 1 Distance between electrode tips on fused images and MRI. Distances in millimeter (standard deviations in brackets) as measured on fused images and postoperative MRI and differences between the two methods

	Fused images	MRI	Difference
Axial plane	22.5 (2.19)	22.3 (2.04)	0.17 (0.49)
Coronal plane	22.6 (2.17)	22.2 (2.11)	0.38 (0.57)

Table 2 Distance of electrode tips to anatomical landmarks on fused images and MRI. Distances in millimeter (standard deviation in brackets) on fused images and postoperative MRI and differences between the two methods

	Fused images	MRI	Difference	p value
Mediolateral				
R electrode	11.5 (1.64)	11.4 (1.42)	0.11 (0.78)	0.5092
L electrode	10.9 (0.94)	11.0 (1.22)	−0.17 (0.73)	0.2655
Craniocaudal				
R electrode	6.5 (1.88)	5.8 (1.56)	0.73 (0.86)	0.0005
L electrode	6.4 (1.34)	5.4 (1.37)	0.97 (0.96)	0.0001
Anteroposterior				
R electrode	3.04 (1.69)	2.38 (1.47)	0.67 (1.27)	0.0199
L electrode	3.09 (1.20)	2.58 (1.31)	0.51 (0.97)	0.0184

The differences found between measures on fused CT/MR images and MR-only images were not statistically significant in the axial plane, while they were for those in the sagittal plane, which concurs with findings in the literature [12]. This may in part be due to differences in identification of the electrode tip center on CT and MRI. The artifact created by the DBS electrode on MRI is larger [13, 14] than that on CT and is not concentric around the actual electrode [8, 12, 14]. Identification of the electrode tip center is thus rendered difficult, especially in vertical planes. In addition, the anatomical distortion on MRI created by susceptibility artifacts [15, 16] may render measures in proximity to the electrode less reliable and explain differences in regard to CT. On the other hand, CT reformations in coronal and sagittal planes imply the risk of artifacts (particularly step artifacts) harboring inaccuracies concerning measures realized in those planes. One drawback of our study was the non-homogeneous CT acquisition protocol (with slice thickness varying between 0.6 and 1.25 mm), although measures realized on images with thicker slices did not show greater errors. Slight inaccuracies of measures realized on postoperative MRIs may also result from the use of a 3D T1 GRE sequence which was not isovoxel (voxel size 0.9×1.28×0.9 mm), chosen because it was less artifacted and its quality most uniform across patients. Finally, even if image alignment on fused images is visually satisfactory, imperfect fusion may play a part in differing results between measures on fused and single-technique images.

The fusion of postoperative CT and postoperative MRI images allows a direct comparison of electrode trajectory and position with possible direct measurements of distances between electrodes, avoiding the comparison of measurements carried out on two different datasets (fused CT/MR images and postoperative MRI) with possible measurement errors in each set. However, the risk of registration errors would persist (as for other fused images), as well as difficulties in exact electrode tip identification. Taking into account the

anatomical distortion in proximity to the electrodes on MRI and the small deviations of electrode position on MRI and CT, differences would be difficult to evaluate reliably.

Measures realized in this study were carried out in regard to "simple" anatomic lines, i.e., midline and AC-PC line, and not in regard to the target structures (STN), as it was designed for a rapid assessment of the accuracy of measures realized on fused images as compared to the current imaging standard (MRI). As fusion appears to function with acceptable results, it could permit a more precise analysis of electrode tip position, namely in relation to anatomical landmarks and target sites as well as cartesian coordinates. Exact verification of electrode position in relation to target and surrounding structures can provide information and explanations for clinical (side) effects and lead to therapeutic adjustments, such as the choice of the most appropriate electrode contact for stimulation. This can be useful for subcortical structures such as the STN, the thalamus and the pallidum targeted for different indications (e.g., PD, dystonia, essential tremor, epilepsy), as in a study where STN DBS stimulation parameters were changed based on the information on electrode position provided by the fusion of preoperative MRI and CT acquired 6 months after DBS surgery [17]. It may also serve for the analysis of electrode position in relation to cortical targets in epilepsy, concerning superficial and deep electrodes implanted in the workup of epilepsy [18] as well as in DBS, with analysis of the distance between electrode contacts and the estimated ictal focus [19].

Apart from avoiding the risks connected to postoperative MRI, the rapid acquisition of CT as compared to MRI improves patient comfort and diminishes risks of potential motion artifacts. The use of a software installed on a radiological workstation allows rapid image analysis and availability.

Conclusions

Fusion of CT and MRI images provides a safe and fast technique for postoperative assessment of electrode position in DBS.

Acknowledgments Statistical support was provided by Professor Thomas Perneger, Clinical Research Center, University of Geneva and Geneva University Hospitals.

Ethical standards and patient consent We declare that all human studies have been approved by the Geneva Ethics Committee and have therefore been performed in accordance with the ethical standards laid down in the 1964 Declaration of Helsinki and its later amendments. We declare that all patients gave informed consent prior to inclusion in this study.

Conflict of interest We declare that we have no conflict of interest.

References

1. Benabid AL, Pollak P, Gervason C, Hoffmann D, Gao DM, Hommel M, Perret JE, de Rougemont J (1991) Long-term suppression of tremor by chronic stimulation of the ventral intermediate thalamic nucleus. Lancet 337(8738):403–406
2. Benabid AL, Pollak P, Louveau A, Henry S, de Rougemont J (1987) Combined (thalamotomy and stimulation) stereotactic surgery of the VIM thalamic nucleus for bilateral Parkinson disease. Appl Neurophysiol 50(1–6):344–346
3. Volkmann J (2007) Update on surgery for Parkinson's disease. Curr Opin Neurol 20(4):465–469. doi:10.1097/WCO.0b013e32816f76ca
4. Spiegel J, Fuss G, Backens M, Reith W, Magnus T, Becker G, Moringlane JR, Dillmann U (2003) Transient dystonia following magnetic resonance imaging in a patient with deep brain stimulation electrodes for the treatment of Parkinson disease. Case report. J Neurosurg 99(4):772–774. doi:10.3171/jns.2003.99.4.0772
5. Henderson JM, Tkach J, Phillips M, Baker K, Shellock FG, Rezai AR (2005) Permanent neurological deficit related to magnetic resonance imaging in a patient with implanted deep brain stimulation electrodes for Parkinson's disease: case report. Neurosurgery 57(5): E1063, discussion E1063
6. Larson PS, Richardson RM, Starr PA, Martin AJ (2008) Magnetic resonance imaging of implanted deep brain stimulators: experience in a large series. Stereotact Funct Neurosurg 86((2):92–100. doi:10.1159/000112430
7. Weise LM, Schneider GH, Kupsch A, Haumesser J, Hoffmann KT Postoperative MRI examinations in patients treated by deep brain stimulation using a non-standard protocol. Acta Neurochir (Wien) 152 (12):2021–2027. doi:10.1007/s00701-010-0738-y
8. Pinsker MO, Herzog J, Falk D, Volkmann J, Deuschl G, Mehdorn M (2008) Accuracy and distortion of deep brain stimulation electrodes on postoperative MRI and CT. Zentralbl Neurochir 69(3): 144–147. doi:10.1055/s-2008-1077075
9. Ferroli P, Franzini A, Marras C, Maccagnano E, D'Incerti L, Broggi G (2004) A simple method to assess accuracy of deep brain stimulation electrode placement: pre-operative stereotactic CT+postoperative MR image fusion. Stereotact Funct Neurosurg 82(1):14–19. doi:10.1159/000076655-76655
10. O'Gorman RL, Jarosz JM, Samuel M, Clough C, Selway RP, Ashkan K (2009) CT/MR image fusion in the postoperative assessment of electrodes implanted for deep brain stimulation. Stereotact Funct Neurosurg 87(4):205–210. doi:10.1159/000225973
11. Shin M, Lefaucheur JP, Penholate MF, Brugieres P, Gurruchaga JM, Nguyen JP (2007) Subthalamic nucleus stimulation in Parkinson's disease: postoperative CT-MRI fusion images confirm accuracy of electrode placement using intraoperative multi-unit recording. Neurophysiol Clin 37(6):457–466. doi:10.1016/j.neucli.2007.09.005
12. Yoshida F, Miyagi Y, Morioka T, Hashiguchi K, Murakami N, Matsumoto K, Nagata S, Sasaki T (2008) Assessment of contact location in subthalamic stimulation for Parkinson's disease by co-registration of computed tomography images. Stereotact Funct Neurosurg 86(3):162–166. doi:10.1159/000120428
13. Yelnik J, Damier P, Demeret S, Gervais D, Bardinet E, Bejjani BP, Francois C, Houeto JL, Arnule I, Dormont D, Galanaud D, Pidoux B, Cornu P, Agid Y (2003) Localization of stimulating electrodes in patients with Parkinson disease by using a three-dimensional atlas-magnetic resonance imaging coregistration method. J Neurosurg 99(1):89–99. doi:10.3171/jns.2003.99.1.0089
14. van Rooijen BD, Backes WH, Schijns OE, Colon A, Hofman PA Brain imaging in chronic epilepsy patients after depth electrode (stereoelectroencephalography) implantation: magnetic resonance

imaging or computed tomography? Neurosurgery 73 (3):543–549. doi:10.1227/01.neu.0000431478.79536.68

15. Kondziolka D, Dempsey PK, Lunsford LD, Kestle JR, Dolan EJ, Kanal E, Tasker RR (1992) A comparison between magnetic resonance imaging and computed tomography for stereotactic coordinate determination. Neurosurgery 30(3):402–406, discussion 406–407
16. Sumanaweera TS, Adler JR Jr, Napel S, Glover GH (1994) Characterization of spatial distortion in magnetic resonance imaging and its implications for stereotactic surgery. Neurosurgery 35(4):696–703, discussion 703–694
17. Lee JY, Jeon BS, Paek SH, Lim YH, Kim MR, Kim C Reprogramming guided by the fused images of MRI and CT in subthalamic nucleus stimulation in Parkinson disease. Clin Neurol Neurosurg 112 (1):47–53. doi:10.1016/j.clineuro.2009.10.008
18. Darcey TM, Roberts DW Technique for the localization of intracranially implanted electrodes. J Neurosurg 113 (6):1182–1185. doi:10.3171/2009.12.JNS091678
19. Bondallaz P, Boex C, Rossetti AO, Foletti G, Spinelli L, Vulliemoz S, Seeck M, Pollo C Electrode location and clinical outcome in hippocampal electrical stimulation for mesial temporal lobe epilepsy. Seizure 22 (5):390–395. doi:10.1016/j.seizure.2013.02.007